

# Copolymerization of styrene and acrylonitrile in ternary oil-in-water microemulsions

K. C. Lee, L. M. Gan and C. H. Chew

Department of Chemistry, National University of Singapore, Singapore 0511,  
Republic of Singapore

and S. C. Ng\*

Department of Physics, National University of Singapore, Singapore 0511, Republic of  
Singapore

(Received 15 June 1994)

The monomer reactivity ratios of styrene–acrylonitrile (SAN) copolymerization in microemulsions, evaluated from  $^{13}\text{C}$  n.m.r. spectroscopic analysis, were found to be variables which not only vary with the feed molar ratio of styrene to acrylonitrile but actually depend on the molar ratio of monomers in the microenvironment of the polymerization loci. The copolymerization loci were found to be the microemulsion droplets. The calculated compositions of the SAN copolymers based on the monomer reactivity ratios that were obtained were in good agreement with the experimental values determined by elemental analysis. The glass transition temperatures of the SAN copolymers were found to decrease linearly with the increasing mole fraction of styrene in the copolymers.

(Keywords: microemulsion; copolymerization; monomer reactivity ratio)

## INTRODUCTION

The homopolymerization of microemulsions<sup>1–9</sup> has been extensively investigated since 1980. In contrast, little attention has been paid to the study of the copolymerization of microemulsions. In water-in-oil (w/o) microemulsion copolymerization, Candau *et al.*<sup>10,11</sup> showed that the reactivity ratios for the copolymerization of both of the water-soluble monomers acrylamide ( $M_1$ ) and sodium acrylate ( $M_2$ ) in inverse microemulsions were close to unity. These values are significantly different from those reported in the literature ( $r_1 \sim 0.95$ ;  $r_2 \sim 0.30$ ) obtained from copolymers prepared in solution or in an inverse emulsion. In our recent work on the copolymerization of styrene and methyl methacrylate<sup>12</sup> in ternary oil-in-water (o/w) microemulsions it has also been demonstrated that the monomer reactivity ratios ( $r_S = 0.74 \pm 0.09$  and  $r_M = 0.38 \pm 0.04$ ) obtained from microemulsion copolymerization were different from those obtained from bulk copolymerization ( $r_S = 0.50$  and  $r_M = 0.45$ )<sup>13</sup>. This difference is attributed to the rather high solubility (1.56 wt%) of methyl methacrylate (MMA)<sup>14</sup> in the aqueous phase.

In this paper, in order to study the effect of monomer solubility on the monomer reactivity ratios, a monomer, namely acrylonitrile (AN), with a water solubility higher than that of MMA, was used to copolymerize with styrene in ternary o/w

microemulsions. Acrylonitrile can dissolve in amounts as high as 7.35 wt%<sup>14</sup> in water.

## EXPERIMENTAL

### Materials

Tetradecyltrimethylammonium bromide (TTAB) purchased from Tokyo Chemical Industry was recrystallized from an ethanol–acetone mixture. Potassium persulfate (KPS) (from Fluka) was recrystallized from doubly distilled water. Styrene and acrylonitrile (AN) (both from Fluka) were purified by vacuum distillation (3 mmHg at 20°C).

### Copolymerization

Microemulsion copolymerizations were carried out at 60°C using 0.15 mM of KPS. The compositions of the microemulsions were 7 wt% mixed monomers (varying the feed molar ratio of the styrene and AN monomers), 9 wt% TTAB and 84 wt% water. The copolymer samples at low conversion (below 8%) were precipitated by a large quantity of methanol. They were purified by repeated washing with methanol and were then vacuum dried for 24 h.

### Copolymer characterization

The compositions of the copolymers were determined by elemental analysis, while the monomer reactivity ratios were evaluated by  $^{13}\text{C}$  n.m.r. spectroscopic analysis. The 125 MHz  $^{13}\text{C}$  n.m.r. spectra were recorded

\* To whom correspondence should be addressed

with a Bruker AMX 500 spectrometer using the WALTZ-16 decoupling procedure at 298 K. Sample concentrations were ca. 5% (wt/vol) in  $\text{CDCl}_3$  solution. The spectra were run at a  $45^\circ$  pulse angle, with a 5 s pulse

**Table 1** Compositions of styrene and acrylonitrile (AN) in the feeds and copolymers<sup>a</sup>

System	$f_s^b$	$f_{AN}^c$	$F_s^d$	$F_{AN}^e$	Conversion (%)
SAN10	0.90	0.10	0.87	0.13	2.13
SAN25	0.75	0.25	0.80	0.20	2.04
SAN50	0.50	0.50	0.69	0.30	2.30
SAN60	0.40	0.60	0.67	0.33	7.57
SAN75	0.25	0.75	0.63	0.37	6.54
SAN90	0.10	0.90	0.53	0.47	7.82

<sup>a</sup> Microemulsion compositions: 9 wt% TTAB, 84 wt% water, 7 wt% of mixed styrene and AN with various molar ratios and 0.15 mM KPS. Polymerization temperature =  $60^\circ\text{C}$

<sup>b</sup> Mole fraction of styrene in the feed

<sup>c</sup> Mole fraction of AN in the feed

<sup>d</sup> Mole fraction of styrene in the copolymer

<sup>e</sup> Mole fraction of AN in the copolymer

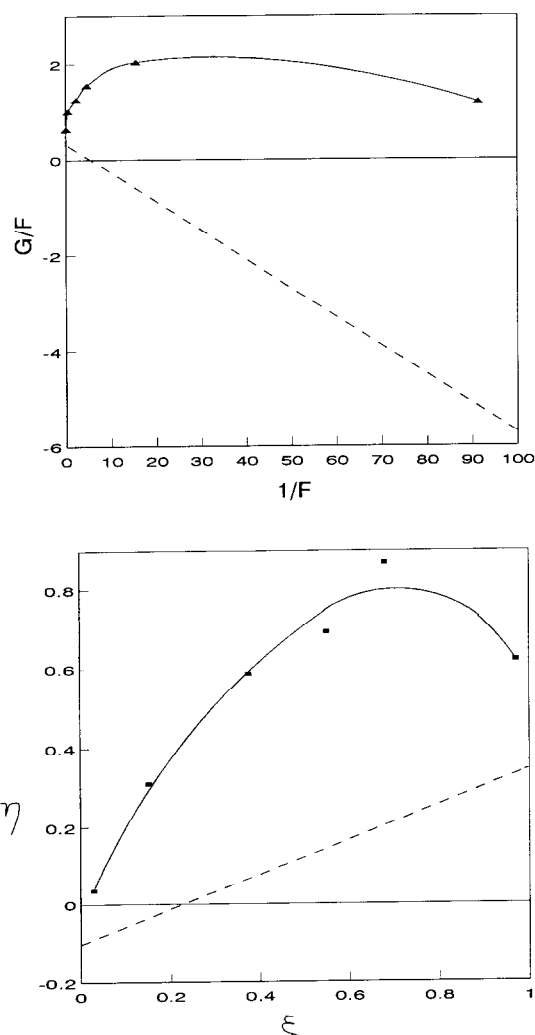


**Figure 1** Fineman–Ross (a) and Kelen–Tudos (b) plots for the SAN system; the solid lines represent experimental values, while the dashed lines are calculated values based on  $r_s = 0.34$  and  $r_{AN} = 0.06$

recycle time, to ensure that all of the carbon-13 nuclei had completely relaxed. Spectra were obtained by accumulating for 5000–8000 scans.

The glass transition temperatures ( $T_g$ )s of the copolymers were measured by using a Perkin–Elmer DSC-4 Differential Scanning Calorimeter with a heating rate of  $20^\circ\text{C min}^{-1}$ . The initial onset of the slope of the differential scanning calorimetry (d.s.c.) curve was taken as the  $T_g$ .

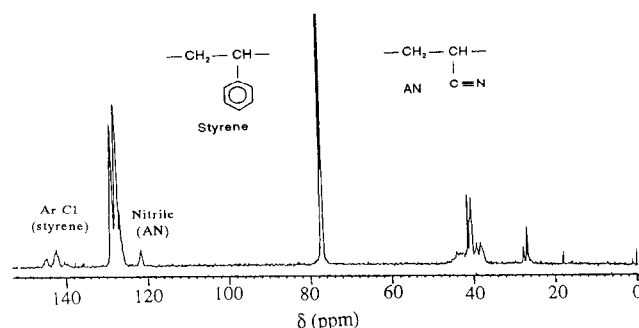
## RESULTS AND DISCUSSION

### Composition of SAN copolymers

The compositions of the styrene–acrylonitrile (SAN) copolymers determined by elemental analysis are shown in Table 1, together with the compositions of styrene and AN in the feeds. According to the Fineman–Ross<sup>15</sup> and Kelen–Tudos<sup>16</sup> graphical methods, linear plots should be obtained based on the composition data. However, as shown in Figure 1, both the Fineman–Ross and Kelen–Tudos plots are curves rather than straight lines. The experimental curves are totally different from the theoretical plots (dashed lines) which were evaluated using the monomer reactivity ratios ( $r_s = 0.34$  and  $r_{AN} = 0.06$ ) obtained by bulk polymerization<sup>17,18</sup>. This deviation is much more serious than that found in the styrene–MMA systems<sup>12</sup>. The high solubility of the AN monomer in the aqueous phase could cause this marked deviation. The solubility of the AN monomer in water (7.35 wt%) is much higher than that of the MMA monomer (1.56 wt%)<sup>14</sup>. A substantial difference between the monomer molar ratios in the microenvironment of the polymerization loci and the feed ratios is expected for the styrene–acrylonitrile microemulsion system. As a result, the monomer reactivity ratios for styrene and AN in microemulsions could not be deduced from either the Fineman–Ross or the Kelen–Tudos plots because no linear relationship can be established.

### Monomer reactivity ratios and microstructures of SAN copolymers from $^{13}\text{C}$ n.m.r. spectroscopic analysis

A  $^{13}\text{C}$  n.m.r. spectrum of a SAN copolymer is presented in Figure 2. The aromatic C1 region (chemical shift,  $\delta = 146.8$ – $138.7$  ppm) and nitrile carbon region ( $\delta = 122.5$ – $118.0$ ) were used for analysis. Expanded aromatic C1 regions and nitrile carbon regions of the studied SAN copolymers are shown in Figure 3. The assignments of the resonances of the AN- and styrene-centred triads are as follows: SSS

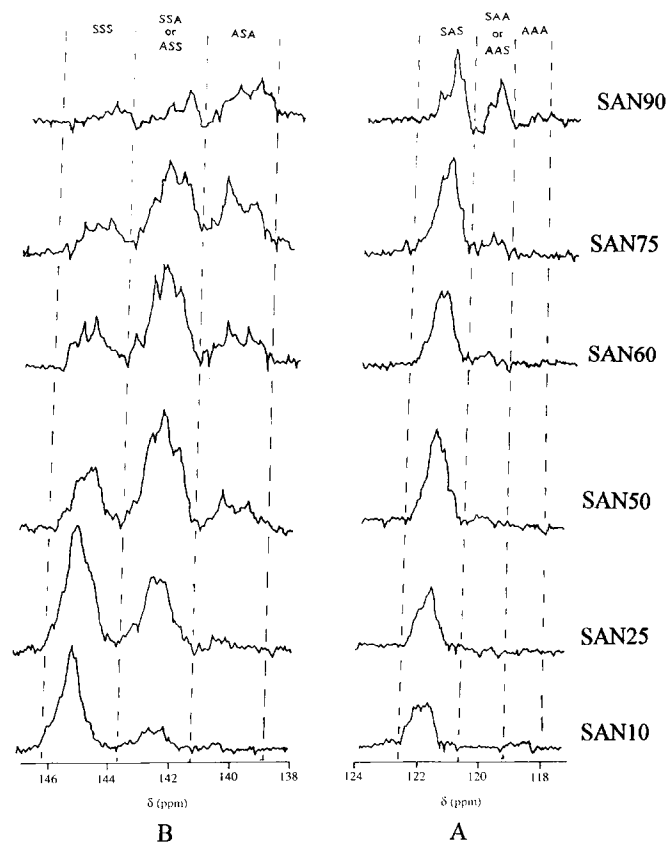


**Figure 2**  $^{13}\text{C}$  n.m.r. spectrum of a SAN50 copolymer in  $\text{CDCl}_3$  at 298 K

**Table 2** Calculated and observed fractions of styrene- and acrylonitrile (AN)-centred triads in SAN copolymers

System	Styrene-centred triads			AN-centred triads			Type <sup>a</sup>
	$F_{SSS}$	$F_{SSA}$	$F_{ASA}$	$F_{AAA}$	$F_{AAS}$	$F_{SAS}$	
SAN10	0.57	0.37	0.06	0.00	0.01	0.99	Calculated
	0.73	0.22	0.04	0.00	0.01	0.99	Observed
SAN25	0.25	0.50	0.25	0.00	0.04	0.96	Calculated
	0.55	0.38	0.07	0.00	0.01	0.99	Observed
SAN50	0.06	0.38	0.56	0.00	0.11	0.89	Calculated
	0.27	0.56	0.16	0.00	0.03	0.97	Observed
SAN60	0.03	0.30	0.67	0.01	0.15	0.84	Calculated
	0.25	0.53	0.22	0.00	0.04	0.96	Observed
SAN75	0.01	0.18	0.81	0.02	0.26	0.72	Calculated
	0.18	0.49	0.33	0.00	0.05	0.95	Observed
SAN90	0.00	0.07	0.93	0.12	0.46	0.42	Calculated
	0.13	0.24	0.63	0.00	0.31	0.69	Observed

<sup>a</sup> The calculated fractions obtained for the triads were based on the monomer reactivity ratios obtained by bulk copolymerization, i.e.  $r_S = 0.34$ , and  $r_{AN} = 0.06$

**Figure 3** Expanded  $^{13}\text{C}$  n.m.r. spectra of SAN copolymers: (A) nitrile carbon regions; (B) aromatic C1 regions

( $\delta = 146.8\text{--}143.7$  ppm), SSA or ASS ( $\delta = 143.7\text{--}141.2$  ppm), ASA ( $\delta = 141.2\text{--}138.7$  ppm), SAS ( $\delta = 122.5\text{--}120.8$  ppm), SAA or AAS ( $\delta = 120.8\text{--}119.2$  ppm) and AAA ( $\delta = 119.2\text{--}118.0$  ppm). These assignments are based on those reported by Schaefer<sup>19</sup>, Arita *et al.*<sup>20</sup> and Hill *et al.*<sup>21</sup>.

The triads distributions determined from Figure 3 are summarized in Table 2. Theoretical predictions of the

styrene- and AN-centred triads which were calculated based on the monomer reactivity ratios obtained by bulk polymerization ( $r_S = 0.34$  and  $r_{AN} = 0.06$ )<sup>17,18</sup> and the Alfrey–Mayo model<sup>22</sup> are also included in Table 2 for comparison. It can be seen that the experimental results are totally different from the predicted values. For instance, the experimental values of all the  $F_{SSS}$  parameters are much higher than the respective calculated ones. This implies that the molar ratios of the styrene and AN present in the polymerization loci of the o/w microemulsion systems are higher than the corresponding feed ratios. Therefore the monomer reactivity ratios obtained from bulk or homogeneous copolymerizations cannot be applied to the copolymerization of styrene and AN in o/w microemulsions.

The monomer reactivity ratios can be evaluated from the  $^{13}\text{C}$  n.m.r. spectra of the SAN copolymers by using the triad distribution data as follows<sup>23</sup>:

$$r_S = \frac{f_{AN}}{f_S} \left( \frac{1}{P_{(A/S)}} - 1 \right)$$

$$r_{AN} = \frac{f_S}{f_{AN}} \left( \frac{1}{P_{(S/A)}} - 1 \right)$$

where

$$P_{(S/A)} = \frac{F_{SAS} + F_{SAA}/2}{F_{AAA} + F_{AAS} + F_{SAS}}$$

$$P_{(A/S)} = \frac{F_{ASA} + F_{SSA}/2}{F_{SSS} + F_{SSA} + F_{ASA}} \quad (1)$$

and  $f_{AN}$  and  $f_S$  are the feed ratios of AN and styrene, respectively.

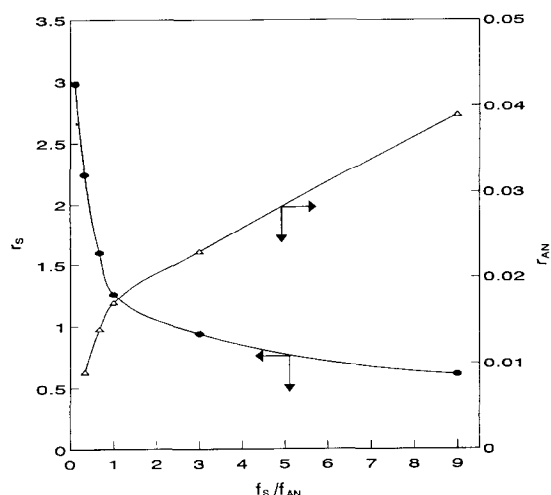
The monomer reactivity ratios of  $r_S$  and  $r_{AN}$  for microemulsion copolymerization are related to those found for bulk or solution copolymerizations,  $r'_S$  (0.34) and  $r'_{AN}$  (0.06)<sup>17,18</sup>, as follows<sup>24</sup>:

$$r_S = r'_S k_{SA}; \quad r_{AN} = r'_{AN} / k_{SA}$$

$$f'_S / f'_{AN} = k_{SA} (f_S / f_{AN}) \quad (2)$$

**Table 3** The monomer reactivity ratios ( $r_S$  and  $r_{AN}$ ) evaluated from  $^{13}\text{C}$  n.m.r. spectroscopic data for the copolymerization of styrene and acrylonitrile in microemulsions

System	$f_S/f_{AN}$	$r_S$	$r_{AN}$
SAN10	9.00	0.61	0.039
SAN25	3.00	0.94	0.023
SAN50	1.00	1.26	0.017
SAN60	0.67	1.60	0.014
SAN75	0.33	2.24	0.009
SAN90	0.11	2.98	$\sim 0$

**Figure 4** The variations of  $r_S$  and  $r_{AN}$  with the feed molar ratios of styrene to AN ( $f_S/f_{AN}$ )

where  $f_S/f_{AN}$  is the molar ratio of styrene/AN in the feed, while  $k_{SA}$  and  $f'_S/f'_{AN}$  are, respectively, the distribution coefficient and the molar ratio of styrene/AN in the polymerization loci.

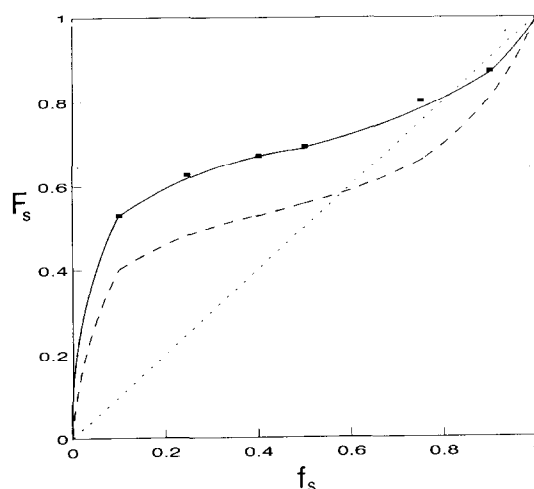
Table 3 summarizes the calculated values of  $r_S$  and  $r_{AN}$ . These values are not constant but vary with the molar ratio of  $f_S/f_{AN}$ , as shown in Figure 4. It can be seen that  $r_S$  decreases, while  $r_{AN}$  increases, with the increasing feed molar ratio  $f_S/f_{AN}$ . The continuous decrease of  $r_S$  and increase of  $r_{AN}$  are due to the variation of the distribution coefficient of styrene-AN ( $k_{SA}$ ) at different feed molar ratios. Based on these different monomer reactivity ratios, values of  $k_{SA}$  were calculated using equation (2) and the results are summarized in Table 4, together with their average values.

Using the average values of  $k_{SA}$ , the molar ratios of styrene to AN in the polymerization loci ( $f'_S/f'_{AN}$ ) were calculated and these are summarized in Table 5. These ratios are indeed much higher than the feed molar ratios ( $f_S/f_{AN}$ ), due to a much higher solubility of AN (7.35 wt%) than that of styrene (0.031 wt%) in the aqueous phase. This implies that the copolymerization loci are the microemulsion droplets.

The amounts of AN in the polymerization loci (microemulsion droplets) and the aqueous phase were also calculated with the assumption that an insignificant amount of the added styrene was dissolved in the aqueous phase. As shown in Table 5, the calculated concentration of AN in the aqueous phase increases from 0.28 to 5.58 wt% when the charged concentration of AN increases from 0.70 to 6.30 wt%. It can also be

**Table 4** The distribution coefficients of styrene-AN ( $k_{SA}$ ) evaluated from the monomer reactivity ratios of styrene and acrylonitrile in microemulsion copolymerization

System	$k_{SA}$ (Styrene)	$k_{SA}$ (AN)	$k_{SA}$ (Average)
SAN10	1.79	1.54	1.67
SAN25	2.76	2.61	2.68
SAN50	3.70	3.62	3.66
SAN60	4.70	4.39	4.55
SAN75	6.58	6.54	6.56
SAN90	8.77	—	8.77

**Figure 5** Monomer-copolymer composition curve for SAN copolymer:  $f_S$ , mole fraction of styrene;  $F_S$ , mole fraction of styrene in copolymer. The solid curve represents calculated values based on monomer reactivity ratios deduced from  $^{13}\text{C}$  n.m.r. spectroscopic data, the dashed curve represents calculated values based on  $r_S = 0.34$  and  $r_{AN} = 0.06$ , while the squares are experimental results obtained from elemental analysis; the dotted line represents ideal random copolymerization

seen that the ratio of the feed AN dissolving in the aqueous phase to the charged AN increases from 0.4 to 0.89. This means the solubility of AN increases with the increasing feed concentration of AN. Hence, it is the variation of the partitioning of AN in the microemulsion droplets and in the aqueous phase that causes the monomer reactivity ratios to change as functions of the feed AN.

In order to further confirm the reliability of the monomer reactivity ratios evaluated from  $^{13}\text{C}$  n.m.r. spectroscopy, copolymer compositions were calculated based on these monomer reactivity ratios and the results are compared with those obtained from elemental analysis (Table 6). The calculated copolymer compositions based on the monomer reactivity ratios ( $r_S = 0.34$ ,  $r_{AN} = 0.06$ ) obtained from bulk copolymerization are also included for comparison. It can be clearly seen that the experimental results obtained from elemental analysis are very similar to those values calculated using the monomer reactivity ratios obtained by spectroscopy, but not those calculated using the ratios obtained from bulk polymerization. This also confirms the assertion that the monomer reactivity ratios for the copolymerization of styrene and AN in o/w microemulsions are not constant.

Figure 5 illustrates the monomer-copolymer composition curves of styrene-AN copolymerization. This shows

**Table 5** The calculated values of the molar ratio of styrene to AN in the polymerization loci ( $f'_S/f'_{AN}$ ) and the amount of AN dissolved in the aqueous phase, based on the values of  $k_{SA}$  given in Table 4

System	$f_S/f_{AN}$	$f'_S/f'_{AN}$	$f'_{AN}$	$f_{AN} - f'_{AN}$	AN dissolved in aqueous phase (wt%)	AN charged (wt%)	AN (Aq.)
							AN (charged)
SAN10	9.00	14.98	0.06	0.04	0.28	0.70	0.40
SAN25	3.00	8.04	0.09	0.16	1.10	1.75	0.63
SAN50	1.00	3.65	0.14	0.36	2.55	3.50	0.73
SAN60	0.67	3.03	0.13	0.47	3.28	4.20	0.78
SAN75	0.33	2.16	0.11	0.64	4.46	5.27	0.85
SAN90	0.11	0.98	0.10	0.80	5.58	6.30	0.89

**Table 6** Comparison between copolymer compositions obtained from elemental analysis and values calculated from n.m.r. spectroscopy and bulk copolymerization data

System	Elemental analysis data			Calculated data <sup>a</sup>			Calculated data <sup>b</sup>		
	$F_S$	$F_{AN}$	$F_S/F_{AN}$	$F_S$	$F_{AN}$	$F_S/F_{AN}$	$F_S$	$F_{AN}$	$F_S/F_{AN}$
SAN10	0.87	0.13	6.75	0.87	0.13	6.50	0.80	0.20	4.06
SAN25	0.80	0.20	4.02	0.79	0.21	3.78	0.66	0.34	1.98
SAN50	0.69	0.30	2.26	0.68	0.31	2.22	0.56	0.47	1.26
SAN60	0.67	0.33	2.04	0.67	0.33	2.03	0.53	0.47	1.13
SAN75	0.63	0.37	1.67	0.63	0.37	1.69	0.48	0.52	0.94
SAN90	0.53	0.47	1.13	0.53	0.47	1.12	0.40	0.60	0.67

<sup>a</sup> Based on monomer reactivity ratios, obtained from microemulsion copolymerization, evaluated from <sup>13</sup>C n.m.r. spectroscopic data<sup>b</sup> Based on monomer reactivity ratios obtained from bulk copolymerization<sup>17,18</sup>**Table 7** Reactivity ratios of styrene-acrylonitrile copolymerization involving different polymerization methods

Polymerization method	Reactivity ratios		Ref.
	$r_S$	$r_{AN}$	
Bulk	0.34	0.06	17, 18
Bulk	$0.331 \pm 0.27-0.42$	$0.053 \pm 0.04-0.07$	21
Bulk	0.41	0.04	20
Solution	0.34	0.13	25
Solution	0.46	0.07	26
Solution	0.43	0.03	26
Microemulsion	$(0.61-2.98)^a$	$(0.009-0.039)^a$	This work

<sup>a</sup> Varies with the feed molar ratios of styrene/acrylonitrile

excellent agreement between the experimental results (squares) and the calculated results for microemulsion copolymerization (solid line). However, the calculated results based on the monomer reactivity ratios obtained from bulk copolymerization data (dashed line) differ substantially. The azeotrope composition shifts from 0.58 for bulk copolymerization to 0.82 for microemulsion copolymerization of styrene-AN, as indicated in Figure 5 by the respective intersections of the dotted line (ideal random copolymerization) with the dashed and solid lines.

The monomer reactivity ratios for styrene-AN copolymerization obtained from different methods of copolymerization are summarized in Table 7. The reactivity ratios for bulk and solution copolymerizations are quite similar. On the other hand, due to the prominent partitioning effect of the AN monomer in the microemulsions (discussed above), the monomer

**Table 8** Copolymerization parameters of styrene-acrylonitrile copolymers

System	$F_{SS}$	$F_{SA}$	$F_{AA}$	$N_S$	$N_A$	$K$	$R$
SAN10	0.74	0.26	0.00	6.46	1.00	1.17	26.33
SAN25	0.59	0.41	0.00	3.81	1.00	1.28	40.82
SAN50	0.39	0.61	0.01	2.25	1.02	1.43	60.97
SAN60	0.35	0.65	0.01	2.07	1.02	1.47	64.72
SAN75	0.27	0.72	0.01	1.74	1.03	1.55	72.46
SAN90	0.13	0.79	0.07	1.33	1.18	1.60	79.47

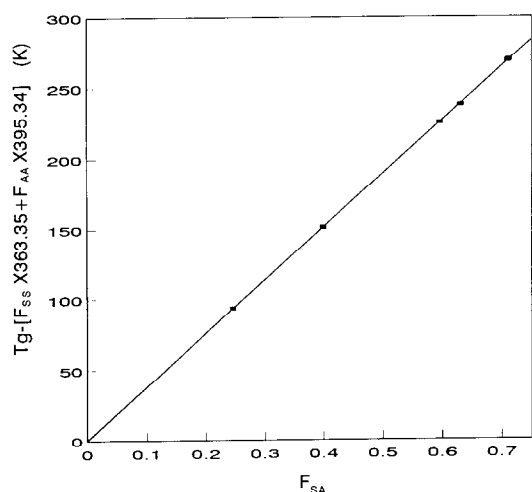
reactivity ratios vary with the feed molar ratio in microemulsion copolymerization. This clearly shows that the copolymerization loci (microenvironment) for styrene and AN in microemulsions are different from those in bulk and solution copolymerizations.

#### Number-average sequence length, block character and run number

Table 8 shows the diad distributions ( $F_{SS}$ ,  $F_{SA}$  and  $F_{AA}$ ) which were calculated using the diad-triad relationship<sup>22</sup> and the number-average sequence lengths ( $N_S$  and  $N_A$ ) which were evaluated from the triad distributions<sup>22</sup>. It can be seen that sample SAN10 has the highest  $F_{SS}$  due to the highest concentration of styrene used. However, for sample SAN90,  $F_{AA}$  is very low (0.07) due to the partitioning effect of AN and the low  $r_{AN}$ . However, its alternating diad ( $F_{SA}$ ) is the highest. The  $N_S$  value which gives the styrene monomer units in a styrene segment decreases from 6.5 to 1.3, while the  $N_A$  value shows that there is about one AN monomer unit in each AN segment for the copolymers. In addition, the block character<sup>23</sup> ( $K$ ) and run number<sup>23</sup> ( $R$ ) were

**Table 9** Glass transition temperature ( $T_g$ ) values for the SAN copolymers

System	$T_g^a$ (K)	$T_g^b$ (K)
SAN10	367.65	367.26
SAN25	369.92	369.44
SAN50	372.81	372.52
SAN60	373.26	373.55
SAN75	375.35	374.75
SAN90	378.67	378.12

<sup>a</sup> Experimental values<sup>b</sup> Values calculated from Barton equation<sup>27</sup>**Figure 6** The plot of  $[T_g - (F_{SS}T_{g,SS} + F_{AA}T_{g,AA})]$  vs.  $F_{SA}$  for SAN copolymers; the line is a linear least-squares fit

calculated and are also included in Table 8. The values of  $K$  show that the SAN copolymer shifts towards a more alternating nature as the feed molar ratio of styrene to AN decreases. The value of  $R$ , which gives the number of segments per hundred monomer units, increases continuously from 26 to 79 as the AN concentration increases from samples SAN10 to SAN90.

#### Glass transition temperature

The measured  $T_g$  values for the SAN copolymers are listed in Table 9. These values decrease linearly with the increase in  $F_S$ . The  $T_g$  of polyacrylonitrile ( $T_{g,AA}$ ) and polystyrene ( $T_{g,SS}$ ) were evaluated from the intercepts of  $T_g$  vs.  $F_S$  at  $F_S = 0$  and  $F_S = 1$ , respectively, to give the following results:  $T_{g,AA} = 395.34$  K and  $T_{g,SS} = 363.35$  K. Barton<sup>27</sup> has suggested that the  $T_g$  is affected by the sequential distribution of monomeric units of a linear copolymer, and is given by the following equation:

$$T_g = F_{SS}T_{g,SS} + F_{AA}T_{g,AA} + F_{SA}T_{g,SA} \quad (3)$$

where  $T_{g,SA}$  is the  $T_g$  of the styrene–AN diad sequence.

The plot of  $T_g - (F_{SS}T_{g,SS} + F_{AA}T_{g,AA})$  vs.  $F_{SA}$ , shown in Figure 6, yields a straight line. The value of 377.85 K ( $T_{g,SA}$ ) obtained from the slope of the line was used to predict the  $T_g$  values of the SAN copolymers that were studied, according to the Barton equation. Table 9 shows that the experimental and calculated  $T_g$  values are in good agreement.

## CONCLUSIONS

The monomer reactivity ratios of the monomer pairs copolymerized in o/w microemulsions are not necessarily constant but depend on the actual molar ratio of the monomers in the microenvironment of the polymerization loci. The molar ratio of the monomers present is governed by the different solubilities of the monomers in the aqueous phase. The deviations from linear Fineman–Ross and Kelen–Tudos plots observed for the microemulsion copolymerization of styrene and acrylonitrile are due to the high solubility of acrylonitrile in the aqueous phase.

The molar ratios of styrene to acrylonitrile in the microenvironment of the polymerization loci are always higher than the initial feed ratios, implying that the copolymerization predominantly proceeds in the microemulsion droplets. The solubility of acrylonitrile in the aqueous phase varies with the feed molar ratios. This variation of the partitioning of acrylonitrile in the microemulsion droplets and in the aqueous phase causes the monomer reactivity ratios of the styrene–acrylonitrile copolymerization in microemulsions to depend strongly on the feed molar ratio of the monomers.

## REFERENCES

- 1 Leong, Y. S. and Candau, F. J. *J. Phys. Chem.* 1982, **86**, 2269
- 2 Candau, F. J., Leong, Y. S. and Fitch, R. M. *J. Polym. Sci. Polym. Chem. Edn* 1985, **23**, 193
- 3 Atik, S. S. and Thomas, J. K. *J. Am. Chem. Soc.* 1981, **103**, 4279
- 4 Tang, H. I., Johnson, P. L. and Gulari, E. *Polymer* 1984, **25**, 1357
- 5 Johnson, P. L. and Gulari, E. *J. Polym. Sci. Polym. Chem. Edn* 1984, **22**, 3967
- 6 Guo, J. S., El-Aasser, M. S. and Vanderhoff, J. W. *J. Polym. Sci. Polym. Chem. Edn* 1989, **27**, 691
- 7 Gan, L. M., Chew, C. H., Lee, K. C. and Ng, S. C. *Polymer* 1993, **34**, 3064
- 8 Gan, L. M., Chew, C. H., Lim, J. H., Lee, K. C. and Gan, L. H. *Colloid Polym. Sci.* in press
- 9 Gan, L. M., Chew, C. H., Lee, K. C. and Ng, S. C. *Polymer* in press
- 10 Candau, F., Zekhnini, Z. and Heatley, F. *Macromolecules* 1986, **19**, 1895
- 11 Candau, F., Zekhnini, Z., Heatley, F. and Franta, E. *Colloid Polym. Sci.* 1986, **264**, 676
- 12 Gan, L. M., Lee, K. C., Chew, C. H., Ng, S. C. and Gan, L. H. *Macromolecules* submitted
- 13 Uebel, J. J. and Dinan, F. J. *J. Polym. Sci. Polym. Chem. Edn* 1983, **21**, 2427
- 14 Riddick, A. J., Bunger, W. B. and Sakano, J. K. 'Organic Solvents', Vol. II, 4th Edn, Wiley, New York, 1986
- 15 Fineman, M. and Ross, S. D. *J. Polym. Sci.* 1950, **5**, 269
- 16 Kelen, T. and Tudos, F. *J. Macromol. Sci. Chem.* 1975, **9**, 1
- 17 Thompson, B. R. and Raines, R. H. *J. Polym. Sci.* 1959, **41**, 265
- 18 Pichot, C., Zaganianis, E. and Guylot, A. *J. Polym. Sci. Polym. Symp. Edn* 1975, **52**, 55
- 19 Schaefer, J. *Macromolecules* 1971, **4**, 107
- 20 Arita, K., Ohtomo, T. and Tsurumi, Y. *J. Polym. Sci. Polym. Lett. Edn* 1981, **19**, 211
- 21 Hill, D. J., O'Donnell, J. H. and O'Sullivan, P. W. *Macromolecules* 1982, **15**, 960
- 22 Koenig, J. L. 'Chemical Microstructure of Polymer Chains', Wiley, New York, 1980, Ch. 3
- 23 Brar, A. S. and Sunita, J. *J. Polym. Sci. Polym. Chem. Edn* 1992, **30**, 2549

- 24 Wall, F. T., Florin, R. E. and Delbecq, C. J. *J. Am. Chem. Soc.* 1950, **72**, 4769
- 25 Guyot, A., Guillet, J., Pichot, C. and Guerrero, L. R. in 'Emulsion Polymers and Emulsion Polymerization' (eds D. R. Bessett and A. E. Hamielec), ACS Symposium Series, American Chemical Society, Washington, DC, 1981, Ch. 26
- 26 Asakura, J. I., Yoshihara, T. and Maeshima, T. *J. Macromol. Sci. Chem.* 1981, **15**, 1473
- 27 Barton, J. M. *J. Polym. Sci. (Part C)* 1970, **30**, 573